

Model of Film Condensation on a Vertical Plate with Noncondensing Gas

David Naylor* and Jacob Friedman†
Ryerson University, Toronto, Ontario M5B 2K3 Canada

DOI: 10.2514/1.43136

An approximate numerical method has been proposed for solving three-dimensional condensation heat transfer on a vertical flat plate in a crossflow of humid air. The external flow of air and water vapor was modeled using an empirical correlation for forced convection over a flat plate with suction. The analogy between heat and mass transfer was used to calculate the local mass transfer rate to the condensate film. For the liquid phase, the heat transfer was calculated as conduction across a falling laminar film, using standard thin-film assumptions. The local Nusselt number distribution predicted with the current approximate method was found to compare well with a computational fluid dynamics solution from the literature. Sample results have been presented for condensation on a vertical plate with freestream temperatures and humidity levels that correspond to the exhaust conditions of a 20 kW industrial clothes dryer.

Nomenclature

D	=	binary diffusion coefficient, m^2/s
g_m	=	local mass transfer coefficient, $\text{kg}/\text{m}^2\text{s}$
H	=	plate height, m
h_{fg}	=	latent heat of vaporization, J/kg
h_x	=	local convective heat transfer coefficient, $\text{W}/\text{m}^2\text{K}$
k	=	thermal conductivity, W/mK
L	=	plate length, m
M	=	molecular mass, kg
m	=	control volume index in y direction
$\dot{m}''_{i,v}$	=	local condensation rate at the interface, $\text{kg}/\text{m}^2\text{s}$
n	=	control volume index in x direction
Nu_x	=	local Nusselt number
\overline{Nu}_x	=	average Nusselt number
Pr	=	Prandtl number
P_{sat}	=	vapor saturation pressure, Pa
P_1	=	total pressure, Pa
q''	=	local heat flux, W/m^2
Re	=	Reynolds number
Sc	=	Schmidt number
Sh	=	Sherwood number
T_i	=	liquid/vapor interface temperature, $^{\circ}\text{C}$
T_w	=	cold wall temperature, $^{\circ}\text{C}$
U_1	=	freestream velocity, m/s
v_i	=	interface velocity (positive in the z direction), m/s
w	=	mass fraction
β_x	=	local suction parameter
Γ	=	mass flow rate of condensate per unit depth, kg/sm
$\Delta\dot{m}_v$	=	vapor condensation rate for the control volume, kg/s
δ	=	local condensate film thickness, m
μ	=	dynamic viscosity, Ns/m^2
ρ	=	density, kg/m^3
ϕ	=	relative humidity

Subscripts

A	=	air
-----	---	-----

film	=	condensate film
i	=	liquid/vapor interface of the condensate film
ℓ	=	liquid water film
v	=	vapor
w	=	cold wall
1	=	freestream conditions

Introduction

FILM condensation in the presence of noncondensable gases has been widely studied for a variety of geometries and flow conditions. This problem is of practical importance for the design of condensers for power plants, refrigeration systems, nuclear safety systems, and various chemical processes. Detailed reviews of the literature have been given by Marto [1] and Carey [2].

Condensation of vapor in the presence of noncondensable gases involves coupled heat and mass transfer. There are two general approaches for solving this class of problem. One method is to use computational fluid dynamics (CFD) to solve the coupled governing equations for heat, mass, and momentum transfer. These equations are solved simultaneously in the liquid film and in the gas flow. In general, this method is difficult to apply because of the vastly different length scales involved. Typically, the liquid condensate film is at least two orders of magnitude thinner than the thermal, momentum, and concentration boundary layers in the gas flow. Also, in a full CFD solution, the location of the liquid/gas interface must be tracked. To the authors' knowledge, commercial CFD codes cannot handle this class of two-phase problem. The CFD solutions currently in the literature have been custom programmed, often using coordinate transformations, and are limited to two-dimensional flow [3,4]. Hence, the designers of heat transfer equipment usually resort to simplified methods, which make use of cross-sectional averaged one-dimensional conservation equations and empirical correlations for the boundary conditions [5–7]. The current paper extends this approximate approach for applications with three-dimensional flows.

As an illustration, the current method has been applied to solve the three-dimensional film condensation on a vertical plate in crossflow. The problem geometry is shown in Fig. 1. Warm humid air flows in the x direction with velocity (U_1), parallel to an isothermal vertical plate, which is cooled to temperature T_w . The plate has height H and depth L in the air flow direction. The plate temperature is below the freestream dew-point temperature, such that a three-dimensional condensate film of water flows in the y direction, under the action of gravity. In the gas flow, concentration, momentum, and thermal boundary layers develop simultaneously in the x direction. These conditions are an idealization of those encountered in condensing

Received 8 January 2009; revision received 3 April 2010; accepted for publication 22 April 2010. Copyright © 2010 by the American Institute of Aeronautics and Astronautics, Inc. All rights reserved. Copies of this paper may be made for personal or internal use, on condition that the copier pay the \$10.00 per-copy fee to the Copyright Clearance Center, Inc., 222 Rosewood Drive, Danvers, MA 01923; include the code 0887-8722/10 and \$10.00 in correspondence with the CCC.

*Department of Mechanical and Industrial Engineering, 350 Victoria Street; dnaylor@ryerson.ca (Corresponding Author).

†Department of Mechanical and Industrial Engineering.

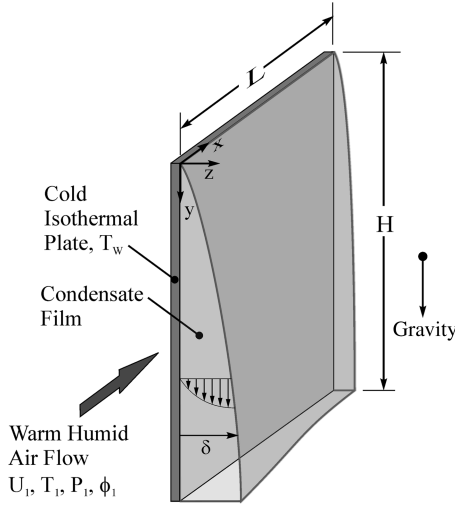


Fig. 1 Problem geometry and coordinate system.

heat exchangers used for air conditioning, heat recovery in furnaces, and other industrial processes.

Simplified Heat and Mass Transfer Model

The current solution procedure is based in part on the method proposed by Rose [8] for solving film condensation on a horizontal plate and the analysis of Maheshwari et al. [5] for solving condensation inside a vertical tube. In the current calculation, the plate is discretized into control volumes, with unequal grid dimensions (Δx and Δy). There were n control volumes in the x direction and m control volumes in the y direction. Over each control volume, a heat balance is applied at the liquid/gas interface of the condensate film. The latent heat transfer rate due to condensation, plus the sensible heat transfer rate to the film surface, is set equal to the heat conduction rate across the laminar liquid film:

$$\Delta Q_{\text{Lat}} + \Delta Q_{\text{Conv}} = \Delta Q_{\text{Cond}}$$

$$\Delta \dot{m}_v h_{fg} + h_x \Delta x \Delta y (T_i - T_w) = k_\ell \Delta x \Delta y \frac{(T_i - T_w)}{\delta} \quad (1)$$

As part of the solution, the liquid/gas interface temperature T_i was calculated iteratively at each control volume to satisfy this heat balance.

The flow in the condensate film was assumed to be laminar, and axial momentum changes within the liquid film were neglected. Viscous shear stress at the liquid/vapor interface has also been neglected. With these standard thin-film assumptions, the local film thickness δ can be expressed in terms of the local mass flow rate of condensate per unit width Γ as follows (Carey [2]):

$$\delta = \left(\frac{3\mu_\ell \Gamma}{\rho_\ell (\rho_\ell - \rho_1) g} \right)^{1/3} \quad (2)$$

In the discretized domain, the local film thickness ($\delta_{n,m}$) was calculated for each column of control volumes by modifying Eq. (2) as follows:

$$\delta_{n,m} = \left(\frac{3\mu_\ell [\Gamma_{n,m-1} + (\Delta \dot{m}_v / 2\Delta x)]}{\rho_\ell (\rho_\ell - \rho_1) g} \right)^{1/3} \quad (3)$$

where

$$\Gamma_{n,m-1} = \frac{1}{\Delta x} \sum_{m=1}^{m-1} \Delta \dot{m}_v$$

In Eq. (3), $\Gamma_{n,m-1}$ is the total condensate mass flow rate for column n , above the control volume of interest. For each column, the calculation was started with $\Gamma = 0$ at the top of the plate and progressed downward. Note that, in Eq. (3), the local condensation

rate for the control volume $\Delta \dot{m}_v$ is divided by two, so that the local film thickness corresponds to the center of the volume. Lateral flow of condensate induced by the crossflow shear stress and surface tension has been neglected. From the perspective of heat transfer design, this is a conservative assumption.

The film Reynolds number was calculated at the bottom of each column of control volumes. In all cases, the local film Reynolds number satisfied the laminar flow criterion (i.e., $Re_{\text{film}} = 4\Gamma_{\text{tot}}/\mu_\ell < 30$). For the range of variables considered in this study, the average value of the film Reynolds number was typically less than 0.5.

Surface condensation produces a bulk velocity of gas toward the wall, as if there was suction at the liquid film interface. Since the liquid phase is impermeable to the noncondensing gas (air), the mass flow rate of air is zero at the interface. So, the air that is carried to the interface by the bulk inward flow must diffuse away from the interface. This requirement can be expressed as

$$-\rho_i D \frac{\partial w_A}{\partial z} \Big|_i = -\rho_{i,A} v_i \quad (4)$$

where v_i is the z component of gas velocity at the interface on the gas side.

Because there is an inward flow at the interface, the mass flux of vapor to the interface $\dot{m}_{i,v}''$ has both a convective and a diffusive component, which can be expressed as follows:

$$\dot{m}_{i,v}'' = -\rho_{i,v} v_i + \rho_i D \frac{\partial w_v}{\partial z} \Big|_i \quad (5)$$

Combining the impermeability condition [Eq. (4)] with Eq. (5) gives the local mass flux of vapor as

$$\dot{m}_{i,v}'' = \frac{g_m (w_{1,v} - w_{i,v})}{(1 - w_{i,v})} \quad (6)$$

In the discretized domain, Eq. (6) was used to calculate the vapor condensation rate over each control volume as follows:

$$\Delta \dot{m}_v = \frac{g_m \Delta x \Delta y (w_{1,v} - w_{i,v})}{(1 - w_{i,v})} \quad (7)$$

Using the condition that the interface is impermeable to the noncondensing gas [Eq. (4)], the interface velocity can be expressed (after some manipulation) as

$$v_i = \frac{-g_m (w_{1,v} - w_{i,v})}{\rho_i (1 - w_{i,v})} \quad (8)$$

Note that the interface velocity is defined as positive in the z direction (i.e., $v_i < 0$).

The mass transfer coefficient (g_m) at the vapor–condensate interface was calculated using the analogy between heat transfer and mass transfer. Rose [8] has shown that the problem of laminar forced convection along a flat plate in the presence of noncondensable gases is identical to laminar forced convection over an isothermal flat plate with suction, where the suction velocity is proportional to $x^{-1/2}$. For the current falling film problem, the condition that $|v_i| \propto x^{-1/2}$ will not be precisely met. However, the interface velocity is small because of the low mass fraction of vapor in the freestream. So, the accuracy of this correction for boundary-layer suction is not critical in this solution.

The correlation for the convective heat transfer on an isothermal plate with suction is given by Rose [9] as

$$Nu_x Re^{-1/2} = \frac{h_x}{k} Re^{-1/2} = \xi(Pr)(1 + 0.941\beta_x^{1.14} Pr^{0.93})^{-1} + \beta_x Pr \quad (9)$$

where

$$\beta_x = -\left(\frac{v_i}{U_1}\right) Re_x^{1/2}; \quad Re_x = \frac{\rho U_1 x}{\mu} \quad (10)$$

and

$$\xi(Pr) = Pr^{1/2}(27.8 + 75.9Pr^{0.306} + 657Pr)^{-1/6}$$

The local mass transfer coefficient g_m at the vapor–condensate interface was calculated using the analogy between heat and mass transfer. In Eqs. (9) and (10), the local Nusselt number was replaced by the local Sherwood number:

$$Sh_x = \frac{g_m x}{\rho D} \quad (11)$$

Also, the Prandtl number was replaced by the Schmidt number:

$$Sc = \frac{\mu}{\rho D} \quad (12)$$

In this manner, Eqs. (9) and (10) were used to calculate both local heat transfer coefficient and the local mass transfer coefficient. The length scale in the Reynolds number was based on the x distance from the leading edge of the plate to the centroid of the control volume. At each control volume, the properties of the humid air were evaluated at the film temperature, $(T_i + T_1)/2$, and at a film vapor pressure.

The water vapor and air densities were calculated assuming an ideal gas mixture. Since saturation conditions exist at the liquid/vapor interface, the mass fraction of vapor at the interface can be expressed as

$$w_{i,v} = \frac{P_{\text{sat}}(T_i)}{P_{\text{sat}}(T_i) + (M_A/M_v)[P_1 - P_{\text{sat}}(T_i)]} \quad (13)$$

where M_A and M_v are the molecular masses of air and water vapor, and $P_{\text{sat}}(T_i)$ is the saturation pressure of the vapor at the interface temperature.

The properties of the condensate film were evaluated at $T_w + (T_i - T_w)/3$, as recommended by Sparrow et al. [10]. The viscosity of the water vapor–air mixture was calculated using the method of Wilke [11]. The thermal conductivity of the mixture was calculated using the method of Friend and Adler [12]. The binary diffusion coefficient D was evaluated as a function of temperature, using the expression recommended by Fujii et al. [13]:

$$D = \frac{7.65 \times 10^{-5}}{P_1} T^{11/6} \quad (14)$$

where P_1 is the total pressure (in pascals) and T is the temperature (in Kelvins). The diffusion coefficient was reevaluated for each control volume at $(T_i + T_1)/2$.

The heat balance [Eq. (1)] and local film thickness [Eq. (3)] have been solved iteratively at each control volume, using Eqs. (7–14). A solution procedure that is easy to program is shown in a flowchart in Fig. 2. To get the calculation started, an initial guess is needed for the liquid/vapor interface temperature and the interfacial gas velocity v_i . It is convenient to use the converged values from the control volume above the current control of interest. The heat transfer and mass transfer coefficients can be calculated from the correlations. Since these coefficients depend (weakly) upon v_i , an iteration loop is needed for interfacial gas velocity. The local condensate film thickness can then be calculated, as well as the conduction heat transfer rate across the film, based on the initial guess of the interface temperature. The accuracy of the local heat balance, expressed by Eq. (1), is then checked. If the residual of Eq. (1) is greater than the desired convergence criterion, the interface temperature is corrected using the conduction heat transfer rate across the film and the film thickness. The outer iteration loop is repeated until Eq. (1) is satisfied. The coding of this solution algorithm was confirmed by performing a detailed hand calculation on a low grid ($n = m = 3$).

Before obtaining the final results, tests were conducted to ensure that both iterative convergence and grid independence were obtained. Based on this grid sensitivity testing, subsequent calculations (for $L = 0.3$ m, $H = 0.2$ m) were performed on a uniform grid with $n = 2000$ control volumes in the gas flow direction (x direction) and $m = 50$ control volumes in condensate flow direction (y direction).

Validation of the Code

To the authors' knowledge, there has not been a previous study of three-dimensional condensation on a vertical plate in crossflow. Since direct validation could not be done, a comparison has been made to published data for a closely related problem, shown in Fig. 3. Two-dimensional condensation of a steam–air mixture in a vertical flat plate channel has been solved by Siow et al. [3] using CFD. With minor modifications, the current computer code was adapted to solve this problem. To simulate a vertical flow of gas in the y direction, the local Nusselt and Sherwood numbers were applied at each control volume as a function of y , rather than as a function of x . However, the effects of the axial pressure gradient and changes in the bulk temperature/concentration in the y direction were not incorporated

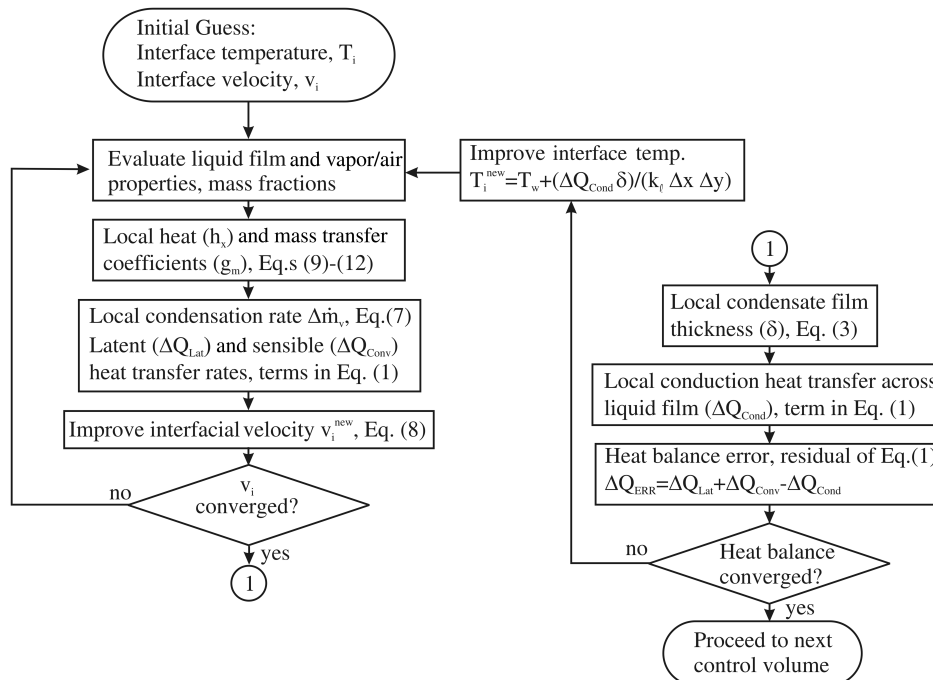


Fig. 2 Solution procedure at each control volume.

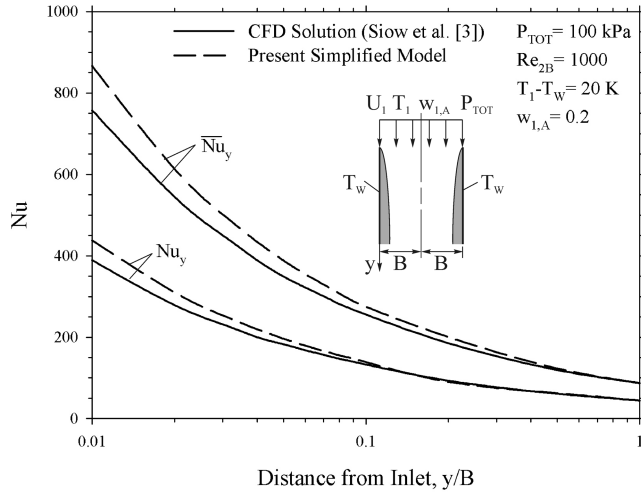


Fig. 3 Comparison of the local and average Nusselt number distributions with the results of Siow et al. [3] for forced convection film condensation of a steam-air mixture at the entrance of a vertical flat plate channel.

into the simplified model. The modified code was, in effect, a model of a vertical isolated plate in a downward flow of gas. Nevertheless, it should be possible to make meaningful comparisons close to the channel inlet, where the heat transfer behavior will be similar to that of an isolated plate.

It should be mentioned that there have been previous studies of two-dimensional condensation on a vertical plate (Shu and Wilks [14,15]). However, these solutions are for a pure saturated vapor without the presence of a noncondensable gas. The noncondensable component greatly suppresses the condensation rate. Depending upon the concentration of the noncondensable gas, the heat transfer rate can be 10 to 100 times lower than for the pure vapor case. For this reason, comparisons have been made with the work of Siow et al. [3], despite the imperfect match of the geometry.

Figure 3 shows the local and average Nusselt number distributions near the inlet ($y/B \leq 1$) of a vertical parallel-plate channel, with a downward-flow steam-air mixture. These results are for an inlet Reynolds number of 10^3 , an inlet gas-to-wall temperature difference of 20 K, and an inlet air mass fraction of 20%. The local and average Nusselt numbers are defined by Siow et al. [3] as

$$Nu_y = \frac{q''_y H}{(T_1 - T_w) k_\ell}; \quad \overline{Nu}_y = \frac{1}{y} \int_0^y Nu_y dy \quad (15)$$

where q''_y is the local heat flux to the plate. It can be seen in Fig. 3 that the local and average Nusselt numbers predicted by the current simplified model are within about 10% of the CFD results of Siow et al. [3]. As mentioned above, perfect agreement would not be expected because of internal flow effects, which have not been modeled. Nevertheless, this comparison provides some confidence in the current solution method.

Sample Results: Heat Recovery from Clothes Dryer Exhaust

Recently, it has been proposed to use a plate heat exchanger to recover the heat from the exhaust stream of industrial clothes dryers. An idealized version of this problem has been used to demonstrate the current method. In the proposed heat exchanger, widely spaced vertical plates would be cooled by the domestic cold water supply, preheating water needed for a wet-wash operation. Sample results are presented for freestream conditions that correspond to the exhaust of a 20 kW clothes dryer: $T_1 = 48.3^\circ\text{C}$, $\phi_1 = 0.9$, and $U_1 = 2.9$ m/s. The calculations have been performed for one side of a single vertical plate with a height of $H = 0.2$ m and a length of $L = 0.3$ m. The plate temperature has been taken as $T_w = 5^\circ\text{C}$, which is the typical

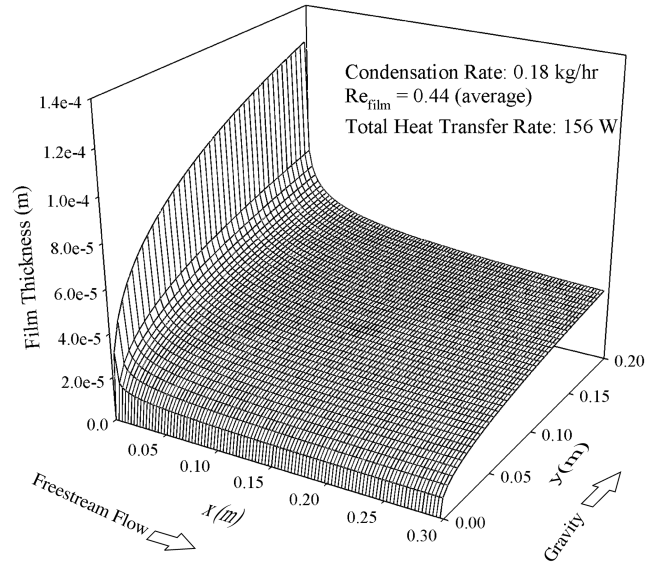


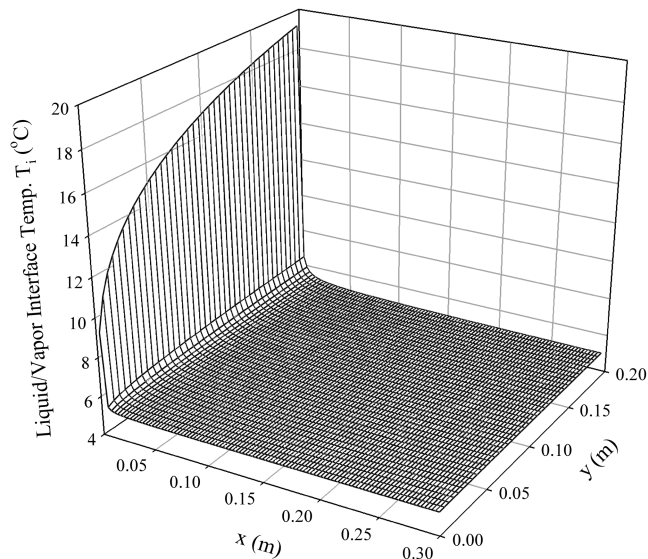
Fig. 4 Surface plot of the condensate film thickness δ ($L = 0.3$ m, $H = 0.2$ m, $T_w = 5.0^\circ\text{C}$, $\phi_1 = 0.9$, $T_1 = 48.3^\circ\text{C}$, $U_1 = 2.9$ m/s, and $P_1 = 100$ kPa).

cold water supply temperature for the winter season in Toronto, Canada.

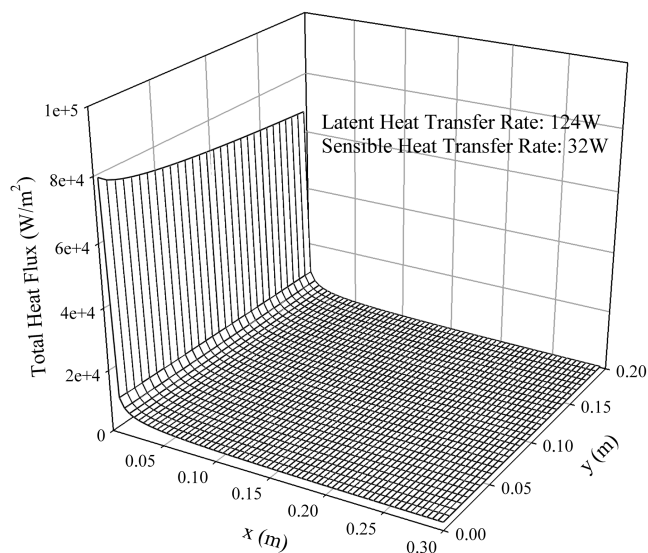
Figure 4 shows the predicted variation of the condensate film thickness δ over the surface of the plate. For this plate length ($L = 0.3$ m), the freestream Reynolds number at the trailing edge of the plate is $Re_L = 5.5 \times 10^4$. So, laminar boundary-layer flow is a reasonable (and conservative) assumption. The liquid film grows in the direction of gravity, reaching a typical thickness of about 0.04 mm at the bottom edge of the plate. As expected, the condensate film thickness increases substantially toward the leading edge because of the high mass transfer coefficient at this location. In fact, it should be mentioned that there is a singularity in the local heat and mass transfer coefficients at the leading edge ($x = 0$) because of the empirical correlations that have been used. So, the numerical calculation was only performed up to $x = 1.5 \times 10^{-4}$ m.

The vapor/liquid interface temperature distribution is shown in Fig. 5a. This temperature distribution is for the same geometry and freestream conditions as in Fig. 4. Over most of the plate, the interface temperature is only slightly higher than the plate temperature, typically about 5.1°C . Given that the freestream dew point temperature is 46.3°C , it can be seen that the dominant thermal resistance is between the freestream and the interface, due to mass transfer effects. Air accumulates at the liquid/vapor interface and suppresses the vapor partial pressure. This suppresses the dew point temperature and mass transfer rate at the interface. In comparison, the thermal resistance of the condensate film is almost negligible, except near the leading edge of the plate ($x \rightarrow 0$). Near the leading edge, the thermal resistance across the condensate layer becomes significant because of the high local mass transfer rate. For these conditions, the conduction resistance across the film increases as the film thickens, causing the interface temperature to increase appreciably in the y direction near the leading edge.

The corresponding variation of the total heat flux over the plate surface is shown in Fig. 5b. Over most of the plate, the heat flux is almost two-dimensional. There is only a slight change in heat flux from the top to the bottom of the plate. For example, consider the local heat flux q'' variation at the trailing edge ($x = 0.3$ m): At $y = 0$, $q'' = 1326.7$ W/m², $y = H = 0.2$ m, and $q'' = 1325.9$ W/m². This result is consistent with the finding that the resistance of the condensate film is small. Since the heat transfer is limited mainly by the mass transfer rate of the vapor to the film, the heat transfer rate takes on almost the same variation as the Sherwood number, which varies only in the x direction. For the conditions shown in Fig. 5b, approximately 20% of the total heat transfer is sensible and 80% is latent. So, this two-dimensional behavior is also reinforced by



a)



b)

Fig. 5 Surface plots of a) the vapor/liquid interface temperature and b) the total heat flux distribution on the plate ($L = 0.3$ m, $H = 0.2$ m, $T_w = 5.0^\circ\text{C}$, $\phi_1 = 0.9$, $T_1 = 48.3^\circ\text{C}$, $U_1 = 2.9$ m/s, and $P_1 = 100$ kPa).

sensible component of heat transfer, which also varies mainly in the x direction.

Conclusions

An approximate numerical model has been proposed for predicting the three-dimensional condensation heat transfer on a vertical plate in a crossflow of humid air. Because this class of problem cannot be readily solved with commercial CFD packages, there is a need for this type of simplified approach. The method described by the authors can be easily self-programmed and is useful for the design purposes.

To illustrate the method, sample results have been presented for condensation on a single vertical plate exposed to a warm humid air stream. In this application, the solution shows that the condensation rate is limited mainly by the mass transfer of vapor from the freestream to the condensate film. The thermal resistance of the condensate film is small, except near the leading edge of the plate.

References

- [1] Marto, P. J., "Condensation," *Handbook of Heat Transfer*, 3rd ed., edited by W. M. Rohsenow, J. P. Hartnett, and Y. I. Cho, McGraw-Hill, New York, 1998, Chap. 14.
- [2] Carey, V. P., *Liquid-Vapor Phase-Change Phenomena*, Taylor and Francis, Bristol, PA, 1992.
- [3] Siow, E. C., Ormiston, S. J., and Soliman, H. M., "A Two-Phase Model For Laminar Film Condensation From Steam-Air Mixtures in Vertical Parallel-Plate Channels," *Heat and Mass Transfer*, Vol. 40, No. 5, 2004, pp. 365–375.
doi:10.1007/s00231-003-0425-0
- [4] Siow, E. C., Ormiston, S. J., and Soliman, H. M., "Fully Coupled Solution of a Two-Phase Model for Laminar Film Condensation of Vapor-Gas Mixtures In Horizontal Channels," *Heat and Mass Transfer*, Vol. 45, No. 18, 2002, pp. 3689–3702.
doi:10.1016/S0017-9310(02)00094-7
- [5] Maheshwari, N. K., Saha, D., Sinha, R. K., and Aritomi, M., "Investigation of Condensation in the Presence of Noncondensable Gas for a Wide Range of Reynolds Number," *Nuclear Engineering and Design*, Vol. 227, No. 2, 2004, pp. 219–238.
doi:10.1016/j.nucengdes.2003.10.003
- [6] Siddique, M., Golay, M. W., and Kazimi, M. S., "Theoretical Modeling of Forced Convection Condensation of Steam in a Vertical Tube in the Presence of a Noncondensable Gas," *Nuclear Technology*, Vol. 106, No. 2, 1994, pp. 202–215.
- [7] No, C. H., and Park, H. S., "Non-Iterative Condensation Modeling for Steam Condensation with Non-Condensable Gas in a Vertical Tube," *International Journal of Heat and Mass Transfer*, Vol. 45, No. 4, 2002, pp. 845–854.
doi:10.1016/S0017-9310(01)00176-4
- [8] Rose, J. W., "Approximate Equations for Forced-Convection Condensation in the Presence of a Non-Condensing Gas on a Flat Plate and Horizontal Tube," *International Journal of Heat and Mass Transfer*, Vol. 23, No. 4, 1980, pp. 539–546.
doi:10.1016/0017-9310(80)90095-2
- [9] Rose, J. W., "Boundary-Layer Flow With Transpiration on an Isothermal Flat Plate," *International Journal of Heat and Mass Transfer*, Vol. 22, No. 8, 1979, pp. 1243–1244.
doi:10.1016/0017-9310(79)90171-6
- [10] Sparrow, E. M., Minkowycz, W. J., and Saddy, M., "Forced Convection Condensation in the Presence of Noncondensibles and Interfacial Resistance," *International Journal of Heat and Mass Transfer*, Vol. 10, No. 12, 1967, pp. 1829–1845.
doi:10.1016/0017-9310(67)90053-1
- [11] Wilke, C. R., "A Viscosity Equation For Gas Mixtures," *Journal of Chemical Physics*, Vol. 18, No. 4, 1950, pp. 517–519.
doi:10.1063/1.1747673
- [12] Friend, L., and Adler, S. B., "Transport Information Needed in the Chemical and Process Industries," *Transport Properties in Gases*, edited by A. B. Cambel, and J. B. Fenn, Northwestern Univ. Press, Evanston, IL, 1988, pp. 124–133.
- [13] Fujii, T., Kato, Y., and Mihara, K., "Expressions of Transport and Thermodynamic Properties of Air, Steam and Water," Univ. of Kyushu Rept. 66, 1977, pp. 81–95.
- [14] Shu, J.-J., and Wilks, G., "Mixed-Convection Laminar Film Condensation on a Semi-Infinite Vertical Plate," *Journal of Fluid Mechanics*, Vol. 300, No. 1, 1995, pp. 207–229.
doi:10.1017/S0022112095003661
- [15] Shu, J.-J., and Wilks, G., "An Accurate Numerical Method for Systems of Differential-Integral Equations Associated with Multi-Phase Flow," *Computers and Fluids*, Vol. 24, No. 6, 1995, pp. 625–652.
doi:10.1016/0045-7930(95)00012-2